Eleonora Guarini ✉ ⓘ ; Ubaldo Bafile ⓘ ; Daniele Colognesi ⓘ ; Alessandro Cunsolo ⓘ ;
Alessio De Francesco ⓘ ; Ferdinando Formisano ⓘ ; Wouter Montfrooij ⓘ ; Martin Neumann ⓘ ;
Fabrizio Barocchi ⓘ

Check for updates

CrossMark

View
Online

Export
Citation

The Journal of Chemical Physics

Special Topic: Adhesion and Friction

Submit Today!

AIP Publishing

Role of the single-particle dynamics in the transverse current autocorrelation function of a liquid metal

View Online   Export Citation   CrossMark

Eleonora Guarini,[1,a] Ubaldo Bafile,[2] Daniele Colognesi,[2] Alessandro Cunsolo,[3]
Alessio De Francesco,[4] Ferdinando Formisano,[4] Wouter Montfrooij,[5] Martin Neumann,[6]
and Fabrizio Barocchi[1]

AFFILIATIONS

[1] Dipartimento di Fisica e Astronomia, Università degli Studi di Firenze, Via G. Sansone 1, I-50019 Sesto Fiorentino, Italy
[2] Consiglio Nazionale delle Ricerche, Istituto di Fisica Applicata "Nello Carrara," Via Madonna del Piano 10,
I-50019 Sesto Fiorentino, Italy
[3] Department of Physics, University of Wisconsin at Madison, 1150 University Avenue, Madison, Wisconsin 53706, USA
[4] CNR-IOM & INSIDE@ILL c/o Operative Group in Grenoble (OGG), F-38042 Grenoble, France and Institut Laue Langevin (ILL),
F-38042 Grenoble, France
[5] Department of Physics and Astronomy, University of Missouri, Columbia, Missouri 65211, USA
[6] Fakultät für Physik der Universität Wien, Kolingasse 14-16, A-1090 Wien, Austria

[a] Author to whom correspondence should be addressed: guarini@fi.infn.it

ABSTRACT

A recent simulation study of the transverse current autocorrelation of the Lennard-Jones fluid [Guarini *et al.*, Phys. Rev. E **107**, 014139 (2023)] revealed that this function can be perfectly described within the exponential expansion theory [Barocchi *et al.*, Phys. Rev. E **85**, 022102 (2012)]. However, above a certain wavevector Q, not only transverse collective excitations were found to propagate in the fluid, but a second oscillatory component of unclear origin (therefore called X) must be considered to fully account for the time dependence of the correlation function. Here, we present an extended investigation of the transverse current autocorrelation of liquid Au as obtained by *ab initio* molecular dynamics in the very wide range of wavevectors $5.7 \leq Q \leq 32.8$ nm^{-1} in order to also follow the behavior of the X component, if present, at large Q values. A joint analysis of the transverse current spectrum and its self-portion indicates that the second oscillatory component arises from the longitudinal dynamics, as suggested by its close resemblance with the previously determined component accounting for the longitudinal part of the density of states. We conclude that such a mode, albeit featuring a merely transverse property, fingerprints the effect of longitudinal collective excitations on single-particle dynamics, rather than arising from a possible coupling between transverse and longitudinal acoustic waves.

Published under an exclusive license by AIP Publishing. https://doi.org/10.1063/5.0152090

I. INTRODUCTION

    Liquid metals have often been regarded as reference systems for investigations of the microscopic dynamics of liquids due to their monatomic nature and the typically sharp features of the dynamic structure factor $S(Q, \omega)$.[1–3] Early studies mainly focused on the characterization of longitudinal collective excitations (often referred to as "sound waves") propagating in these fluids.[3–5] More recently,

experimental and simulation works on the dynamics of liquid metals addressed the behavior of transverse excitations ("shear waves"), certainly present in dense fluids at sufficiently small wavelengths, i.e., above a threshold wavevector Q value that can be as low as a few inverse nanometers, as observed from *ab initio* molecular dynamics (AIMD) simulations of these systems.[6–10] So far, simulations provide the only possibility to determine the most crucial functions for studies of transverse dynamics:[2] the transverse current autocorrelation

function (TCAF) $C_T(Q,t)$ and the velocity autocorrelation function (VAF), here denoted as $Z(t)$. The former probes transverse excitations with varying Q; the latter is, instead, a function of time only and both longitudinal and transverse collective processes contribute to it by affecting the velocity of every single particle. In particular, the spectrum of the VAF $\tilde{Z}(\omega)$ in a liquid is the analog of the phonon density of states (DoS) of a solid, thereby revealing, in an averaged way, all the excitations sustained by the fluid, as shown in the literature both for the model Lennard-Jones (LJ) dense fluid[11] and for liquid metals.[12,13]

Very recently, we demonstrated that by using the exponential expansion theory (EET) of correlation functions,[14–16] a remarkably accurate account of $C_T(Q,t)$ and its spectrum, $\tilde{C}_T(Q,\omega)$, can be obtained for the LJ fluid.[17] In that work, the studied thermodynamic state and Q range permitted an accurate determination of the wavevector at which shear waves start to propagate. Unexpectedly, at higher Q values, we also found that an additional oscillatory contribution had to be considered to properly describe $C_T(Q,t)$. The oscillation frequency of this second component (labeled "X" in Ref. 17) was observed to grow steeply with Q, rapidly overtaking the frequency of transverse waves. The available data, which focused on the low Q range, did not permit any conclusion on the nature and physical meaning of the X contribution to $C_T(Q,t)$. Nonetheless, its frequency ω_X appeared to grow with Q toward the value of the maximum of the dispersion curve of the longitudinal acoustic excitation obtained from $S(Q,\omega)$[11] for the same thermodynamic state of the LJ fluid (see, in particular, the red curve in Fig. 9 of Ref. 11). This fact suggested that the X signal might be a fingerprint in $C_T(Q,t)$ of the longitudinal dynamics.

In order to elucidate the origin of this second phenomenon (X), we turn here to the analysis of $C_T(Q,t)$ of liquid Au as obtained from the simulated atomic configurations already used to calculate both $S(Q,\omega)$[5] and its single-particle (self-)part $S_{self}(Q,\omega)$.[12] The present investigation, extended to Q values well above the position Q_{peak} of the main peak of the static structure factor ($Q_{peak} = 26$ nm^{-1} for Au), enables us to follow the Q dependence of the frequency and damping of the oscillatory processes and to check, in particular, the presence of the X component of $C_T(Q,t)$ in a system substantially different from the LJ fluid.

The choice of Au was suggested not only by the availability of reliable and well-tested[5] AIMD simulations but also, as mentioned, by the enhanced dynamical features typically characterizing correlation functions of liquid metals as compared to other simple fluids. In fact, the sharper spectral features often mitigate interpretative uncertainties. Moreover, the monatomic nature ensures the absence of optic-like (i.e., weakly dispersed) modes that might make the interpretation more complex and allows us to focus solely on acoustic excitations. In addition, we note that monatomic simple liquids can be subdivided into two large categories: noble-gas liquids and liquid metals. While the LJ case already studied is paradigmatic of the first class, it is important to also investigate some representative of the second one in order to check whether certain dynamical features have a "universal" character among simple liquids.

The objective of the present work is to provide a convincing proof of the longitudinal origin of the X component of $C_T(Q,t)$, which not only is detected in the case of simulated Au but is even

more clearly defined than in the LJ system. We will also show that traces of the longitudinal dynamics in a transverse correlation need not necessarily be interpreted as evidence of a mixing, or coupling, of the longitudinal and transverse excitations. This mixing has sometimes been conjectured,[18,19] though never quantitatively demonstrated nor theoretically derived, in order to explain the fact that signs of transverse waves in $S(Q,\omega)$ and of longitudinal waves in $\tilde{C}_T(Q,\omega)$ have been observed in some simulated liquid metals[6–10] or hydrogen bonded liquids.[18,20] More recent studies addressing the mentioned coupling focused on the total current correlation $C_L(Q,t) + 2C_T(Q,t)$,[21,22] showing interesting effects if one starts from a simplified version of both $C_L(Q,t)$ and $C_T(Q,t)$, as constituted by a single oscillatory component. However, the study of the total current is presently not the preferred route in the attempt to explain, as we aim to, the transverse and longitudinal current autocorrelation functions with their clear two-excitation structure above certain Q values. By adopting another point of view, the results of the present study lead us to propose an alternative interpretation, independent of the coupling concept, of the mutual signatures of the main collective processes of fluids in specialized correlation functions, that is, in functions most appropriate to characterize, primarily, either the longitudinal, via $S(Q,\omega)$, or the transverse, through $\tilde{C}_T(Q,\omega)$, excitations. In particular, the self-part of the mentioned autocorrelation functions is shown to contain the traces of all collective processes acting in the fluid and to convey averaged information on the "secondary" ones (transverse or longitudinal, in the above order) to the respective *total* (either longitudinal or transverse) functions, i.e., to $S(Q,\omega)$ and $\tilde{C}_T(Q,\omega)$.

II. BASIC DEFINITIONS AND PRELIMINARY OBSERVATIONS

In a system of N identical monatomic particles, the current $\mathbf{j}$ is defined as $\mathbf{j}(\mathbf{Q},t) = \sum_\alpha \mathbf{v}_\alpha(t)e^{i\mathbf{Q}\cdot\mathbf{R}_\alpha(t)}$, with $\mathbf{R}_\alpha(t)$ and $\mathbf{v}_\alpha(t)$ denoting the position and velocity of the α-th particle. It is usually separated into two parts, $\mathbf{j}_L$ and $\mathbf{j}_T$, where the longitudinal component (parallel to $\mathbf{Q}$) is given by[2]

$$\mathbf{j}_L(\mathbf{Q},t) = (\mathbf{j}(\mathbf{Q},t)\cdot\mathbf{Q})\mathbf{Q}/Q^2, \qquad (1)$$

and the transverse part is simply $\mathbf{j}_T(\mathbf{Q},t) = \mathbf{j}(\mathbf{Q},t) - \mathbf{j}_L(\mathbf{Q},t)$. Following the notation of Ref. 2, the longitudinal current autocorrelation function (LCAF) is then

$$C_L(Q,t) = \frac{1}{N}\langle \mathbf{j}_L^*(\mathbf{Q},0)\cdot\mathbf{j}_L(\mathbf{Q},t)\rangle = -\frac{1}{Q^2}\frac{d^2F(Q,t)}{dt^2}, \qquad (2)$$

where $F(Q,t) = \frac{1}{N}\sum_{\alpha,\beta}\langle e^{-i\mathbf{Q}\cdot\mathbf{R}_\alpha(0)}e^{i\mathbf{Q}\cdot\mathbf{R}_\beta(t)}\rangle$ is the intermediate scattering function. The TCAF is, instead, given by

$$C_T(Q,t) = \frac{1}{2N}\langle \mathbf{j}_T^*(\mathbf{Q},0)\cdot\mathbf{j}_T(\mathbf{Q},t)\rangle. \qquad (3)$$

In Eqs. (2) and (3), $\langle\cdots\rangle$ denotes, as usual, the ensemble average.

By assuming $\mathbf{Q}$ to be parallel to the z-axis, one can also write the LCAF as[2]

$$C_L(Q,t) = \frac{1}{N}\langle j_z^*(\mathbf{Q},0) j_z(\mathbf{Q},t)\rangle$$

$$= \frac{1}{N}\sum_{\alpha\neq\beta}\left\langle v_{z,\alpha}(0) e^{-iQR_{z,\alpha}(0)} v_{z,\beta}(t) e^{iQR_{z,\beta}(t)}\right\rangle$$

$$+ \frac{1}{N}\sum_{\alpha}\left\langle v_{z,\alpha}(0) e^{-iQR_{z,\alpha}(0)} v_{z,\alpha}(t) e^{iQR_{z,\alpha}(t)}\right\rangle$$

$$= C_{L,\text{dist}}(Q,t) + C_{L,\text{self}}(Q,t), \qquad (4)$$

where we introduced the self- and distinct components of the function. An analogous separation can be performed for the TCAF,

$$C_T(Q,t) = \frac{1}{N}\langle j_x^*(\mathbf{Q},0) j_x(\mathbf{Q},t)\rangle$$

$$= \frac{1}{N}\sum_{\alpha\neq\beta}\left\langle v_{x,\alpha}(0) e^{-iQR_{z,\alpha}(0)} v_{x,\beta}(t) e^{iQR_{z,\beta}(t)}\right\rangle$$

$$+ \frac{1}{N}\sum_{\alpha}\left\langle v_{x,\alpha}(0) e^{-iQR_{z,\alpha}(0)} v_{x,\alpha}(t) e^{iQR_{z,\alpha}(t)}\right\rangle$$

$$= C_{T,\text{dist}}(Q,t) + C_{T,\text{self}}(Q,t). \qquad (5)$$

Of course, due to the isotropy of the fluid, one has $C_T(Q,t) = \frac{1}{N}\langle j_x^*(\mathbf{Q},0) j_x(\mathbf{Q},t)\rangle = \frac{1}{N}\langle j_y^*(\mathbf{Q},0) j_y(\mathbf{Q},t)\rangle$.

The velocity autocorrelation function $Z(t)$, whose transform $\tilde{Z}(\omega)$ can be interpreted as the DoS of the fluid, is defined by

$$Z(t) = \frac{1}{N}\sum_{\alpha}\langle \mathbf{v}_\alpha(0)\cdot\mathbf{v}_\alpha(t)\rangle. \qquad (6)$$

Therefore, the comparison of Eqs. (4)–(6) readily shows that, in the $Q \to 0$ limit, the following relations hold:

$$C_{L,\text{self}}(Q\to 0,t) = C_{T,\text{self}}(Q\to 0,t) = \frac{1}{3}Z(t). \qquad (7)$$

As we will show, the self-part of the TCAF has a very weak dependence on Q. As a consequence, $C_T(Q,t)$ contains, in addition to the distinct part, a contribution that is very similar to the VAF, even at nonzero Q values. Consequently, $\tilde{C}_T(Q,\omega)$ has a spectral component that yields the same information as the DoS of the fluid.

It is important to recall that an EET representation of the VAF enables one to distinguish the longitudinal and transverse contributions to the DoS.[12] However, the characteristic frequencies derived from the analysis of the VAF do not correspond, strictly speaking, to those of "propagating collective excitations" with concomitant Q dispersion. In fact, $\tilde{Z}(\omega)$ is independent of Q and has peaks or shoulders at frequencies where the branches of the dispersion relation have a horizontal tangent, as expected from its identification with the density of pseudo-phononic states. For strongly dispersive collective excitations, such as the longitudinal ones, the DoS of a liquid displays a broad shoulder around a frequency corresponding to the maximum of the longitudinal dispersion curve $\omega_s(Q)$ (the subscript "s" meaning "sound") obtained from the analysis of $S(Q,\omega)$.[5,12,13] We show this in Fig. 1 for the case of Au. In this sense, the presence of features in the DoS in some frequency bands, in fact, reveals that longitudinal and transverse branches are present in the dispersion relation and where their average frequency is located. Ultimately, the DoS proves that both sound and shear waves exist in the fluid.

A. Previous results from an EET analysis of $C_T(Q,t)$ of a simple fluid

To provide the background for the present work, we give a brief summary of the exponential expansion formalism[14–16] and of the results obtained with the help of the EET in our recent investigation of $C_T(Q,t)$ in the LJ system.[17]

The exponential expansion theory predicts that any autocorrelation function can be expressed as a series of exponential terms (called *modes*). Thus, at each Q value, $C_T(Q,t)$ can be represented by

$$C_T(Q,t) = C_T(Q,0)\sum_{j=1}^{\infty} I_j \exp(z_j|t|). \qquad (8)$$

In Eq. (8), relaxation processes are accounted for by exponentially decaying terms with real I_j and z_j (with $z_j < 0$), while exponentially damped oscillatory components of the correlation are represented in the series by "complex pairs," i.e., by $I_j\exp(z_j t) + I_j^*\exp(z_j^* t)$ with
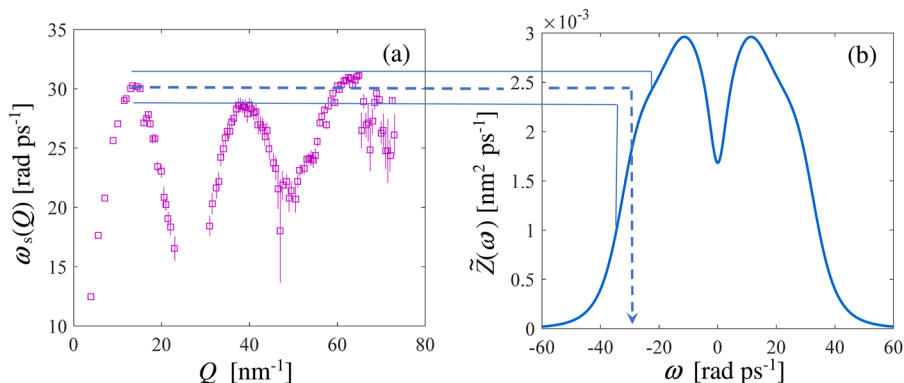
FIG. 1. (a) Longitudinal dispersion curve $\omega_s(Q)$ of liquid Au as obtained from the analysis of the AIMD $S(Q,\omega)$.[5] (b) Spectrum of the VAF (DoS) of liquid Au.[12] The figure shows that the DoS displays a broad shoulder, centered around 30 rad ps^{-1} (dashed arrow), in correspondence with the frequency band (rendered by thin solid lines) approximately containing the maxima of $\omega_s(Q)$.

I_j and z_j complex and Re $z_j < 0$. Note that complex modes appear in conjugate pairs because the correlation is real-valued for classical fluids. In Eq. (8), I_j and z_j are functions of Q, although we omitted this dependence in the above notation.

The EET has enabled very good descriptions of various correlation functions and spectra of interest in studies of the self [11,12] and collective dynamics [13,23] of fluids. Details on its application can be found in Refs. 11–13. In particular, the analysis consists of performing a fitting procedure to determine the parameters z_j and I_j of a small number p of modes to which the sum in Eq. (8), in practice, reduces. Here, we note that a number of $p - 1$ constraints are imposed on the amplitudes I_j in order to enforce the vanishing of the first few odd time derivatives of $C_T(Q, t)$ at $t = 0$. [13]

Application of the above procedure to $C_T(Q, t)$ of the LJ system allowed us to distinguish three wavevector regions where different sets of exponential modes were required to accurately describe the time behavior of the autocorrelation function. In particular, we found that in the rather restricted low-Q range studied, the character of the expansion changes twice, smoothly transitioning from one Q regime to the other. Indeed, pairs of exponential terms may be present in the expansion and describe the time dependence of a component that, depending on its damping, behaves either as an underdamped oscillator with a characteristic frequency or as an overdamped one. On varying Q, such an "oscillator" may smoothly cross the transition between the over- and underdamped states, displaying the onset of a propagating excitation in the fluid. [24]

At the very lowest wavevectors (region I in Ref. 17), three real modes were required to represent the TCAF, one of which perfectly reproduced the Q-dependence of the damping of $C_T(Q, t)$ in the hydrodynamic limit. [2] However, the scheme of the modes was found to change above a transition wavevector (called Q_{gap}) marking the lower boundary of a second dynamical region, thus denoted as II in Ref. 17. In such a region, four modes in total, two real and two complex conjugates, i.e., with Im $z_j \neq 0$, were found to be necessary to attain a very good fit quality. Our analysis showed that the latter complex pair evolves from two out of the three real modes of range I with a transition from an overdamped to an underdamped condition of the kind described above. Such a crossover at Q_{gap} marks the onset of transverse collective

excitations propagating in the fluid. Correspondingly, we denoted the actual oscillation frequency by $\omega_T = \text{Im}\, z_j$ and the damping by $\Gamma_T = -\text{Re}\, z_j$, with the subscript "T" hinting at the transverse character of the parameters of such an oscillator. The so-called undamped frequency, i.e., the frequency the oscillator would have in the ideal case of zero friction, is given by $\Omega_T = \sqrt{\omega_T^2 + \Gamma_T^2}$. Therefore, as far as shear modes were concerned, the picture emerging from $C_T(Q, t)$ was unambiguous. Regarding the remaining two real modes in region II of the LJ system, we observed a larger-Q crossover where these modes also continuously evolve toward the underdamped state of a *second* damped harmonic oscillator, thus defining a third distinctive dynamic region for the processes probed by the TCAF. As stated in Sec. I, given the lack of a precise assignment, in Ref. 17, this second oscillatory term was unspecifically labeled as "X," and its parameters were analogously denoted as ω_X, Γ_X, and $\Omega_X = \sqrt{\omega_X^2 + \Gamma_X^2}$. However, we already noted that the growth of ω_X with increasing Q suggested that it is likely related to the longitudinal dynamics.

III. ANALYSIS OF $C_T(Q, t)$ OF LIQUID Au

The details of the AIMD simulations of liquid Au were given in Ref. 5. Here, we just recall that the simulation was performed with 200 atoms in a cubic box with 1.557 nm edge length, so as to give the atomic number density $n = 53$ nm^{-3} at a temperature $T = 1387$ K, slightly exceeding the melting temperature $T_m = 1337$ K. The above edge length imposes a minimum Q value of 4.0 nm^{-1}. The simulation was first equilibrated in the *NVT* canonical ensemble for 9 ps (3000 steps of 3 fs). The thermalized atom distribution was then simulated in the *NVE* microcanonical ensemble for a duration of 36 ps in 12 000 time steps of 3 fs.

From the atomic configurations, we calculated both $C_{T,L}(Q, t)$ and $C_{T,\text{self}}(Q, t)$ for all wavevectors compatible with the cubic box in the range from $Q_{min} = 4.0$ up to 32.8 nm^{-1}, as well as for the single higher value $Q = 38.1$ nm^{-1}. The limited variation of $C_{T,\text{self}}(Q, t)$, with increasing wavevector is shown in Fig. 2, where we display the self-parts of the LCAF and TCAF at two quite different Q values (4.0 and 25.5 nm^{-1}), along with $Z(t)/3$. At our minimum Q, the self-parts of the current correlations are practically indistinguishable from $Z(t)/3$ [see Eq. (7)]. By contrast, at the higher Q value
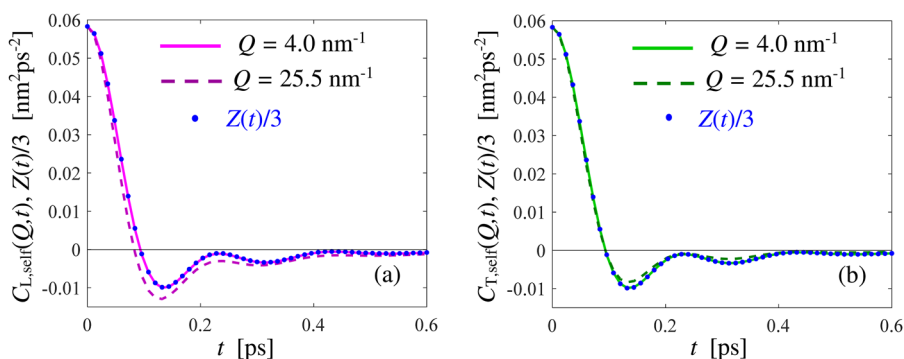
FIG. 2. Time dependence of the self-parts of (a) the longitudinal and (b) the transverse current autocorrelations, compared with $Z(t)/3$ (blue dots). Two Q values are shown for the self-current correlations: 4.0 nm^{-1} (solid) and 25.5 nm^{-1} (dashed).

(25.5 nm^{-1}), we observe that $C_{T,self}(Q,t)$ remains quite close to $Z(t)/3$, while departures are more evident for $C_{L,self}(Q,t)$.

As mentioned above, the simulated $C_T(Q,t)$ was analyzed with an EET model of the form of Eq. (8). Since the minimum set of modes providing a good fit turned out to be $p = 4$ at all investigated wavevectors, the constraints were $\sum_{j=1}^{p} I_j = 1$, which follows directly from Eq. (8) at $t = 0$, $\sum_{j=1}^{p} I_j z_j = 0$, and $\sum_{j=1}^{p} I_j z_j^3 = 0$. The last two conditions enforce the vanishing of the first two odd time derivatives of $C_T(Q,t)$ at $t = 0$, which, in the frequency domain, guarantees that the second and fourth moments of the spectrum $\tilde{C}_T(Q,\omega)$ are finite.

We achieved accurate fits at each available Q value in the range $5.7 < Q < 32.8$ nm^{-1}, while, as often happens at the lowest Q value admitted by the simulation box size, the TCAF at 4.0 nm^{-1} turned out to be affected by the boundary conditions and was difficult to be fitted properly. At the first two wavevector values of the above range, $Q = 5.7$ and 7.0 nm^{-1}, a model containing two real modes and one (low frequency) complex pair accurately described $C_T(Q,t)$ over its entire time range, indicating that shear waves (such as in

region II of Ref. 17) have already set in at the wavevectors probed by the simulations. Conversely, at $Q > 7.0$ nm^{-1}, a satisfactory representation of the data could only be obtained by considering no real modes but two complex pairs, meaning that, just like in the LJ case, a second (underdamped) oscillatory component (labeled as X, for consistency with Ref. 17) contributes to $C_T(Q,t)$, together with the familiar transverse one, labeled as T. Figure 3 provides an example of the quality of the fit to $C_T(Q,t)/C_T(Q,0)$ in this wavevector range.

Figure 4 shows the Q dependence of the actual frequencies $\omega_{T,X}$, damping coefficients $\Gamma_{T,X}$, and undamped frequencies $\Omega_{T,X} = \sqrt{\omega_{T,X}^2 + \Gamma_{T,X}^2}$ of the two contributions to $C_T(Q,t)$. Although the transverse dispersion curve $\omega_T(Q)$ in Fig. 4(a) displays a somewhat noisy behavior, the trend of $\Omega_T(Q)$ in Fig. 4(b) is more regular and resembles that observed in liquid Ag.[7,13] As far as the X pair is concerned, we first note that the initial Q dependence (from 5.7 to, approximately, 15 nm^{-1}) of Ω_X and Γ_X is very much the same as the one found in the underdamped state of the LJ case, namely a nearly flat behavior for the former and a nearly linear decrease in
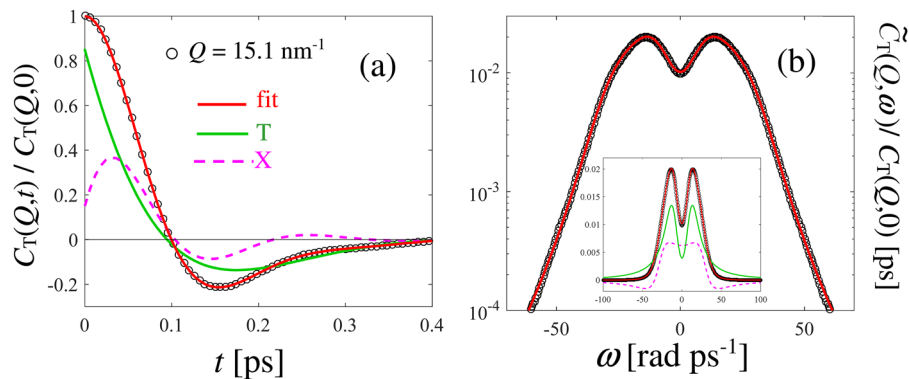
FIG. 3. (a) Normalized $C_T(Q,t)$ of liquid Au at $Q = 15.1$ nm^{-1} (black circles) and fit result (red solid curve). The fit components (two complex pairs) are also shown and specified in the legend. (b) Corresponding spectrum and fit results. The semilogarithmic scale helps appreciate the quality of the fit over more than two decades. The inset shows the spectrum and its components on a linear scale.
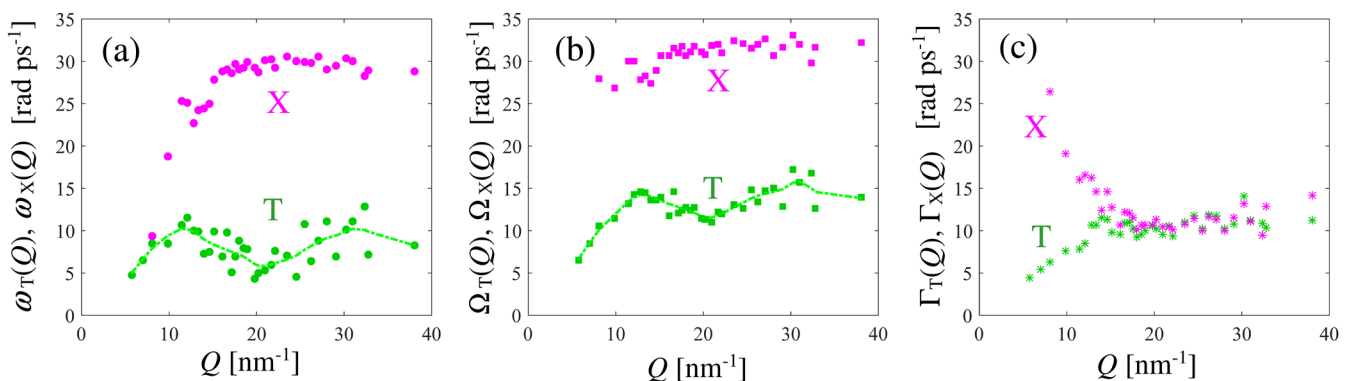
FIG. 4. (a) Q dependence of the frequencies ω_T (green full circles) and ω_X (magenta full circles) as obtained from the fits to $C_T(Q,t)$. The green dotted–dashed spline curve through the T points is just a guide to the eye. (b) Same as panel (a) but for the undamped frequencies Ω_T (green full squares) and Ω_X (magenta full squares). (c) Damping coefficients Γ_T (green asterisks) and Γ_X (magenta asterisks).

the latter. This might suggest that such trends are general and independent of the specific nature of the fluid. It can also be noted that, at $Q \geq 20$ nm^{-1}, Γ_T and Γ_X level off at roughly the same constant value.

The wide Q range considered in the present paper allows us to establish that, after a steep growth, $\omega_X(Q)$ reaches the value of the maximum (30 rad ps^{-1} for Au) of the longitudinal dispersion curve $\omega_s(Q)$ [see Fig. 1(a)]. This behavior could only be guessed at in the LJ case due to the limited Q range covered. Interestingly, here we are able to see that such a frequency value (attained by the X component at $Q \approx 18$ nm^{-1}), which is also the frequency related to the longitudinal processes in the VAF [see Fig. 1(b)], does not change anymore with increasing Q. To further check this constant trend, we also performed a fit to $C_T(Q,t)$ at the single, even higher value of $Q = 38.1$ nm^{-1}, finding (see Fig. 4) for both damping and frequency a behavior similar to that of the preceding Q values. Thus, above 18 nm^{-1}, the behavior of ω_X is not the one expected for a propagating dispersive mode, as confirmed by the results presented in the following.

In Sec. II, we already noted that the second relation in Eq. (7), exact at $Q \to 0$, continues to approximately hold for $C_{T,self}(Q,t)$ also at higher wavevectors (see Fig. 2). On the other hand, we now find that, at $Q > 18$ nm^{-1}, $C_T(Q,t)$ contains an oscillatory component matching the longitudinal complex pair of the VAF reported in Ref. 12. These observations lead us to interpret the X contribution to $C_T(Q,t)$ not only as due to the longitudinal waves propagating in the fluid, in the same way that these excitations contribute to the VAF, but also as representing quite a strong fingerprint in $C_T(Q,t)$ of its own self-part and, thus, ultimately, of the VAF itself. To quantitatively verify this hypothesis, we performed the EET analysis of $C_{T,self}(Q,t)$, described in Sec. IV.

IV. ANALYSIS OF $C_{T,self}(Q,t)$ AND DISCUSSION OF THE RESULTS

For monatomic fluids, the self-part of an autocorrelation function is, in turn, also an autocorrelation function. The EET can then

be applied to self-correlation functions, as already done in Ref. 12. We, thus, modeled $C_{T,self}(Q,t)$ according to

$$C_{T,self}(Q,t) = C_{T,self}(Q,0) \sum_{j=1}^{\infty} I_{j,self} \exp(z_{j,self}|t|) \qquad (9)$$

and performed fits in the same Q range investigated for the total correlation. Given the close resemblance of $C_{T,self}(Q,t)$, with the VAF also at nonzero wavevectors, the model adopted in Ref. 12, consisting of two complex pairs plus one real mode, was also employed here and proved to be very accurate at all wavevectors. Figure 5 shows its performance at a representative Q value. We will indicate the parameters of the low-frequency modes of $C_{T,self}(Q,t)$ with the symbols ω_1 and Γ_1 ($\Omega_1 = \sqrt{\omega_1^2 + \Gamma_1^2}$) and those of the high-frequency complex pair by ω_2 and Γ_2 ($\Omega_2 = \sqrt{\omega_2^2 + \Gamma_2^2}$).

In Fig. 6, the fit results are compared with those of Fig. 4. Very smooth trends of the "self"-parameters are observed, with $\omega_X(Q)$ and $\Gamma_X(Q)$ of $C_T(Q,t)$ nicely falling on top of $\omega_2(Q)$ and $\Gamma_2(Q)$ of $C_{T,self}(Q,t)$ at intermediate and high Q values.[25] Conversely, the transverse dispersion curve $\omega_T(Q)$, and even more so the undamped frequency $\Omega_T(Q)$, as expected, deviate from $\omega_1(Q)$ and $\Gamma_1(Q)$ of the self-correlation function, except at wavevectors exceeding ~25 nm^{-1}.

The two pairs of modes of $C_T(Q,t)$ thus appear to have a profoundly disparate nature, not only because of the different processes they are related to (shear and sound waves) but also because the lower frequency complex pair (the transverse one) embodies, at low and intermediate wavevectors, the genuine collective excitation that the correlation function is suited to reveal, while the other, at almost all Q values, is essentially related to the way in which the existence of longitudinal modes is reflected in the single-particle behavior.

These considerations are also supported by the fact that the distinct part of $C_T(Q,t)$ must play a significant role in the transverse modes over the greatest part of the Q range, giving rise to the weak but visible dispersion of $\omega_T(Q)$ (see Fig. 6). By contrast, the X modes are sensitive to the distinct component only in the first part of the Q range; otherwise, their frequency would differ, also above 18 nm^{-1}, from what is found by the fits to $C_{T,self}(Q,t)$.
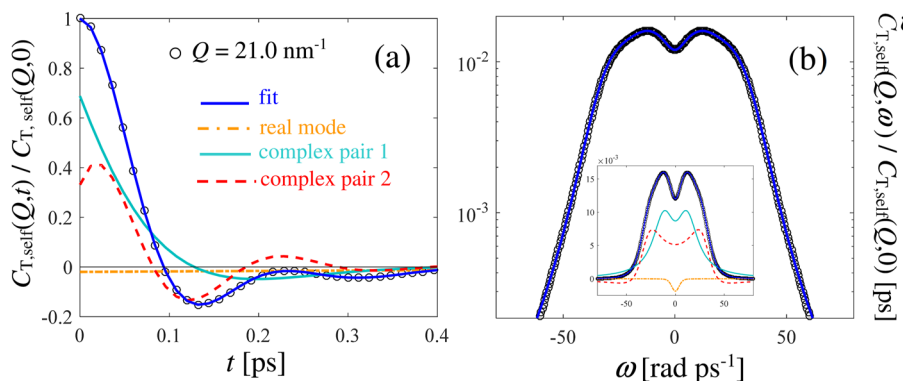
FIG. 5. (a) Normalized $C_{T,self}(Q,t)$ of liquid Au at $Q = 21.0$ nm^{-1} (black circles) and fit result (blue solid curve). The fit components (two complex pairs plus one real mode) are also shown and specified in the legend. (b) Corresponding spectrum and fit results on a semilogarithmic scale. The inset shows the spectrum and all its components on a linear scale.
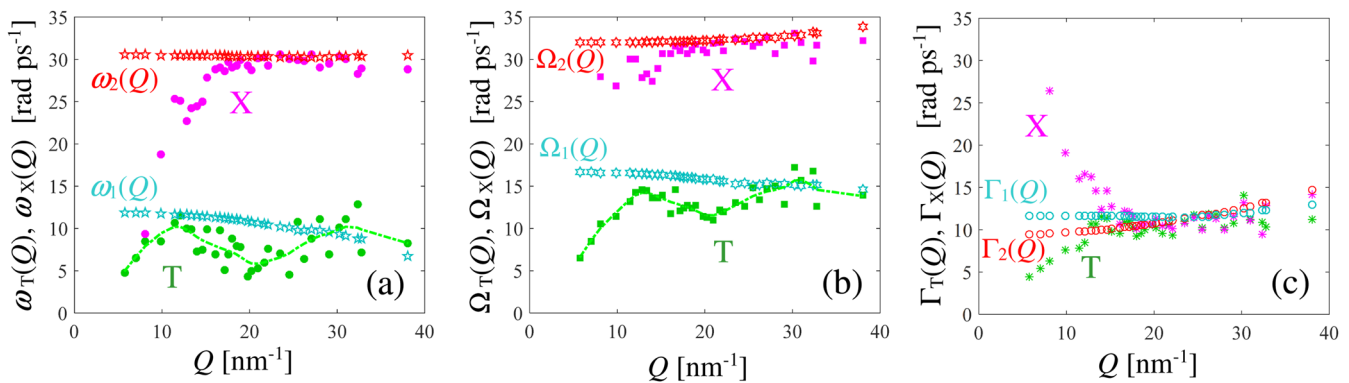
FIG. 6. Same as Fig. 4 with the addition of the results of the fits to $C_{T,self}(Q,t)$. (a) Empty stars are used for the actual frequencies of the complex pairs labeled as 1 (cyan) and 2 (red) in Fig. 5. (b) Same as panel (a) with identical color code. Empty hexagrams represent Ω_1 and Ω_2. (c) Same as panel (b) but for the damping coefficients. Empty circles are used for Γ_1 and Γ_2.

On the other hand, observing that the distinct dynamics mostly affect the transverse excitations means it is primarily the T modes of $C_T(Q,t)$ that embody genuine information about the relative motions of different particles, in agreement with the collective, propagating, and dispersive character we just attributed to these modes of the TCAF.

Nonetheless, even for the T modes of $C_T(Q,t)$, this character is lost above 25 nm^{-1}, where their frequency $\omega_T(Q)$ essentially merges with $\omega_1(Q)$ of Fig. 6(a). We thus conclude that in Au, all the modes here observed lose their collective propagating character above this threshold wavevector. Consequently, at $Q > 25$ nm^{-1}, only the frequencies of $C_{T,self}(Q,t)$, or equivalently of the VAF, can reasonably be found from the analysis of the total correlation $C_T(Q,t)$ as well. *A posteriori*, one realizes that such a collective to single-particle transition in the character of the T component occurs at a Q value corresponding to a distance $(2\pi/Q) \simeq 0.25$ nm, which, at the density of liquid gold, is very close to the average interparticle distance, so that the probed dynamics is essentially that of single atoms. Accordingly, going to smaller (and no longer significant at a "collective level") length scales cannot actually bring new information besides that already contained in the VAF.

For completeness, we report in Fig. 7 the comparison of $C_{T,self}(Q,t)$, and $C_T(Q,t)$ at the three selected wavevectors as $Q = 9.9, 18.5$, and 38.1 nm^{-1}. The first Q value [Fig. 7(a)] belongs to the range where both the T and X components are affected by the distinct part, giving rise to a total correlation that decays and oscillates more slowly than $C_{T,self}(Q,t)$. The second wavevector considered in Fig. 7(b) lies at the beginning of the interval where ω_X reaches and maintains the same constant value of the high-frequency mode of $C_{T,self}(Q,t)$, while the third is the maximum Q investigated in this work. In both the two latter cases [Figs. 7(b) and 7(c)], the very slight difference between the two plotted curves at times longer than 0.1 ps actually does not entail a change of the frequency [see Fig. 6(a)] as determined by the fits to the two functions but only a small, likely not significant, difference in the damping [see Fig. 6(c)].

In this respect, another important remark is suggested by Fig. 8, where the damping derived from the analysis of $S(Q,\omega)$ [here again
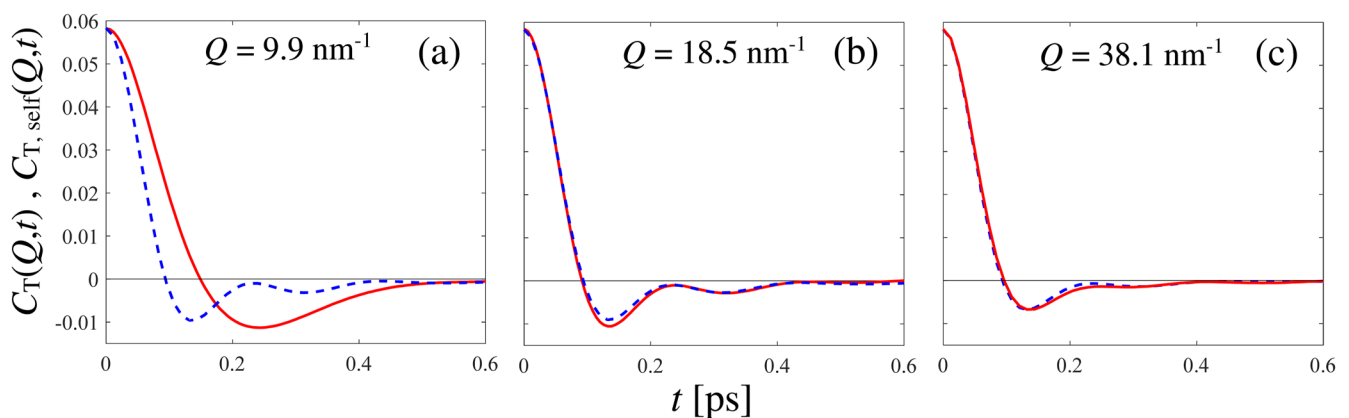
FIG. 7. Total (red solid curve) and self-TCAF (blue dashed curve) at three Q values: (a) 9.9 nm^{-1}, (b) 18.5 nm^{-1}, and (c) 38.1 nm^{-1}.
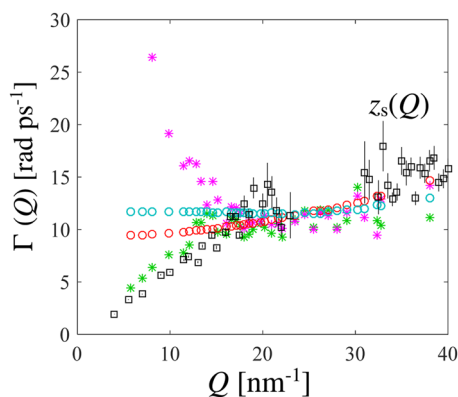
FIG. 8. Same as Fig. 6(c) with the addition of the damping $z_s(Q)$ (black empty squares with error bars) of longitudinal excitations as determined from the dynamic structure factor of liquid Au.[5] The data are missing in the region around $Q_{peak} = 26$ nm^{-1} because, in the propagation gap, where $\omega_s(Q) \rightarrow 0$, fits to $S(Q, \omega)$ become unstable.

indicated as $z_s(Q)$ for consistency with Ref. 5] is superimposed on the results already given in Fig. 6(c). Interestingly, all damping coefficients tend to overlap beyond the well-known "propagation gap" of $\omega_s(Q)$, typically occurring around Q_{peak}, where the static structure factor reaches its maximum.[5] This trend corroborates our overall picture since, at high enough Q values, only a single damping mechanism seems to be detected, whatever dynamical process is investigated through whatever autocorrelation function. Apparently, this is a further proof that, above Q_{peak}, only only the single-particle dynamic behavior is being probed.

V. SYNOPSIS AND FINAL REMARKS

This paper was aimed at providing a quantitative interpretation of an unexpected dynamical feature of the TCAF of fluids we recently found for the LJ system: namely, the existence, along with transverse collective excitations, of another oscillatory component of unclear origin (therefore designated as X) in the correlation. The availability of reliable AIMD simulations for liquid Au allowed us to address the case of a "real" dense fluid and, at the same time, to span a rather wide Q range, where transverse modes have already set in and where the X modes, if present, could be followed appropriately in their evolution with Q.

Our analysis, based on the EET of correlation functions, proved again to be very successful, as in many other cases already reported, and confirmed the presence of the X modes also in $C_T(Q, t)$ of Au, up to the rather high wavevectors of this investigation. The observation of the same phenomenon in such different fluids constitutes, *per se*, an interesting result.

An important clue concerning the nature of the X modes of $C_T(Q, t)$ is given by the almost constant frequency they maintain above a certain Q. In addition, this constant frequency value (30 rad ps^{-1}) turns out to be extremely close to one of the characteristic frequencies found in previous studies on Au, both from the analysis of the VAF and from the maxima of the longitudinal dispersion curve derived from $S(Q, \omega)$.

Since the VAF is a single-particle (self-)property, and the X modes of $C_T(Q, t)$ were observed to have the same characteristics as the longitudinal contribution to the VAF,[12] it was natural to also perform an EET analysis of $C_{T,self}(Q, t)$, given its close resemblance with the VAF at rather high Q values, as shown in Fig. 2. More precisely, although, as Q grows, $C_{T,self}(Q, t)$ does not coincide with the VAF on an absolute scale, it nonetheless displays the presence of longitudinal waves in a fluid in essentially the same way the VAF does and, in particular, with the same frequency, i.e., resulting in a strong similarity in lineshape. We believe that this is not a fortuitous coincidence.

Apart from demonstrating once again the efficacy of the EET in the description of any correlation function, the analysis of $C_{T,self}(Q, t)$ turned out to be essential for proving that the X component of the TCAF, initially of unknown origin, could be unequivocally linked with the single-particle dynamics.

Several other comments, given at the end of Sec. IV, lead to the following conclusive notes:

The TCAF contains two completely distinguishable signatures of the main propagating waves present in a fluid: one provides evidence for the collective transverse excitations (with concomitant Q dispersion) that the function is constructed to detect; the other is essentially a trace of the VAF, embodying information about other (longitudinal) waves in the fluid. It conveys this information in a similar way the DoS does, i.e., without revealing the true dispersion curve $\omega_s(Q)$, except through the more or less marked damping the DoS shows for a specific excitation. In this respect, the behavior of the X mode of $C_T(Q, t)$ at intermediate and high Q values shows that, despite its original designation, such a component is not a new and "unknown propagating collective excitation" emerging in the TCAF but is simply, via $C_{T,self}(Q, t)$, a reflection of the longitudinal contribution to the VAF.

The above observations suggest that what we found for $C_T(Q, t)$ should also hold in the reverse case, where studies of $S(Q, \omega)$ [or equivalently $\tilde{C}_L(Q, \omega)$[26]] show some "transverse-like" contribution to it.[6–10,13] The possibility that such an additional transverse signal to $S(Q, \omega)$ might be due to the self-part was proposed some years ago in the interpretation of simulation data on liquid Na.[27] As a proof of these hypotheses, it would be worth analyzing, quantitatively, i.e., by the EET, the transverse signal and its possible relation with the self-part, also in the case of $S(Q, \omega)$. However, analyses similar to the present one are very demanding and cannot be pursued and described in the same paper. Moreover, given the weakly dispersive character of transverse modes, such an analysis would be far less stringent than the present one.

In conclusion, for simple monatomic liquids, such as LJ and Au, our picture provides an explanation of the observed dynamics independent of possible coupling effects. Rather simply, as this study shows, the self-dynamics emerges in an evident way, bringing to light also those processes that the longitudinal or transverse character of the studied function should, in principle, forbid to observe.

AUTHOR DECLARATIONS

Conflict of Interest

The authors have no conflicts to disclose.

Author Contributions

Eleonora Guarini: Conceptualization (lead); Formal analysis (lead); Investigation (lead); Methodology (equal); Software (lead); Writing – original draft (lead); Writing – review & editing (equal). **Ubaldo Bafile**: Methodology (equal); Writing – review & editing (equal). **Daniele Colognesi**: Methodology (equal); Writing – review & editing (equal). **Alessandro Cunsolo**: Methodology (equal); Writing – review & editing (equal). **Alessio De Francesco**: Methodology (equal); Writing – review & editing (equal). **Ferdinando Formisano**: Methodology (equal); Writing – review & editing (equal). **Wouter Montfrooij**: Methodology (equal); Writing – review & editing (equal). **Martin Neumann**: Methodology (equal); Writing – review & editing (equal). **Fabrizio Barocchi**: Conceptualization (equal); Writing – review & editing (equal).

DATA AVAILABILITY

The data that support the findings of this study are available from the corresponding author upon reasonable request.

REFERENCES

[1] N. H. March, *Liquid Metals* (Cambridge University Press, Cambridge, 1990).

[2] U. Balucani and M. Zoppi, *Dynamics of the Liquid State* (Clarendon, Oxford, 1994).

[3] W. Montfrooij and I. de Schepper, *Excitations in Simple Liquids, Liquid Metals and Superfluids* (Oxford University Press, New York, 2010).

[4] T. Scopigno, G. Ruocco, and F. Sette, "Microscopic dynamics in liquid metals: The experimental point of view," Rev. Mod. Phys. **77**, 881 (2005).

[5] E. Guarini, U. Bafile, F. Barocchi, A. De Francesco, E. Farhi, F. Formisano, A. Laloni, A. Orecchini, A. Polidori, M. Puglini, and F. Sacchetti, "Dynamics of liquid Au from neutron Brillouin scattering and *ab initio* simulations: Analogies in the behavior of metallic and insulating liquids," Phys. Rev. B **88**, 104201 (2013).

[6] M. Marqués, L. E. González, and D. J. González, "*Ab initio* study of the structure and dynamics of bulk liquid Fe," Phys. Rev. B **92**, 134203 (2015).

[7] B. G. del Rio, D. J. González, and L. E. González, "An *ab initio* study of the structure and atomic transport in bulk liquid Ag and its liquid-vapor interface," Phys. Fluids **28**, 107105 (2016).

[8] B. G. del Rio, O. Rodriguez, L. E. González, and D. J. González, "First principles determination of static, dynamic and electronic properties of liquid Ti near melting," Comput. Mater. Sci. **139**, 243 (2017).

[9] B. G. del Rio, L. E. González, and D. J. González, "*Ab initio* study of several static and dynamic properties of bulk liquid Ni near melting," J. Chem. Phys. **146**, 034501 (2017).

[10] B. G. del Rio and L. E. González, "Longitudinal, transverse, and single-particle dynamics in liquid Zn: *Ab initio* study and theoretical analysis," Phys. Rev. B **95**, 224201 (2017).

[11] S. Bellissima, M. Neumann, E. Guarini, U. Bafile, and F. Barocchi, "Density of states and dynamical crossover in a dense fluid revealed by exponential mode analysis of the velocity autocorrelation function," Phys. Rev. E **95**, 012108 (2017).

[12] E. Guarini, S. Bellissima, U. Bafile, E. Farhi, A. De Francesco, F. Formisano, and F. Barocchi, "Density of states from mode expansion of the self-dynamic structure factor of a liquid metal," Phys. Rev. E **95**, 012141 (2017).

[13] E. Guarini, A. De Francesco, U. Bafile, A. Laloni, B. G. del Rio, D. J. González, L. E. González, F. Barocchi, and F. Formisano, "Neutron Brillouin scattering and *ab initio* simulation study of the collective dynamics of liquid silver," Phys. Rev. B **102**, 054210 (2020).

[14] F. Barocchi, U. Bafile, and M. Sampoli, "Exact exponential function solution of the generalized Langevin equation for autocorrelation functions of many-body systems," Phys. Rev. E **85**, 022102 (2012).

[15] F. Barocchi and U. Bafile, "Expansion in Lorentzian functions of spectra of quantum autocorrelations," Phys. Rev. E **87**, 062133 (2013).

[16] F. Barocchi, E. Guarini, and U. Bafile, "Exponential series expansion for correlation functions of many-body systems," Phys. Rev. E **90**, 032106 (2014).

[17] E. Guarini, M. Neumann, A. De Francesco, F. Formisano, A. Cunsolo, W. Montfrooij, D. Colognesi, and U. Bafile, "Onset of collective excitations in the transverse dynamics of simple fluids," Phys. Rev. E **107**, 014139 (2023).

[18] M. Sampoli, G. Ruocco, and F. Sette, "Mixing of longitudinal and transverse dynamics in liquid water," Phys. Rev. Lett. **79**, 1678 (1997).

[19] S. Hosokawa, M. Inui, Y. Kajihara, S. Tsutsui, and A. Q. R. Baron, "Transverse excitations in liquid Fe, Cu and Zn," J. Phys.: Condens. Matter **27**, 194104 (2015).

[20] A. Cunsolo, *The THz Dynamics of Liquids Probed by Inelastic X-Ray Scattering* (World Scientific, Singapore, 2021).

[21] N. P. Kryuchkov, V. V. Brazhkin, and S. O. Yurchenko, "Anticrossing of longitudinal and transverse modes in simple fluids," J. Phys. Chem. Lett. **10**, 4470 (2019), and references therein.

[22] N. P. Kryuchkov, L. A. Mistryukova, V. V. Brazhkin, and S. O. Yurchenko, "Excitation spectra in fluids: How to analyze them properly," Sci. Rep. **9**, 10483 (2019).

[23] E. Guarini *et al.*, "Collective dynamics of liquid deuterium: Neutron scattering and approximate quantum simulation methods," Phys. Rev. B **104**, 174204 (2021).

[24] W. Montfrooij, U. Bafile, and E. Guarini, "Modeling of neutron and x-ray scattering by liquids: The risks of using phenomenological models," Phys. Fluids **33**, 087114 (2021).

[25] Regretfully, we cannot count on an estimate of the errors of the simulation data and, consequently, of the fitted parameters. However, errors can be roughly estimated by looking at the spread of the data points.

[26] It is well known that $\tilde{C}_L(Q, \omega)$ is directly related to $S(Q, \omega)$ [see Eq. (1.148) of Ref. 2] and that an EET description of the two functions provides the same real and complex modes, differing only in their amplitude (see Appendix A of Ref. 13).

[27] G. Garberoglio, R. Vallauri, and U. Bafile, "Time correlation functions of simple liquids: A new insight on the underlying dynamical processes," J. Chem. Phys. **148**, 174501 (2018).